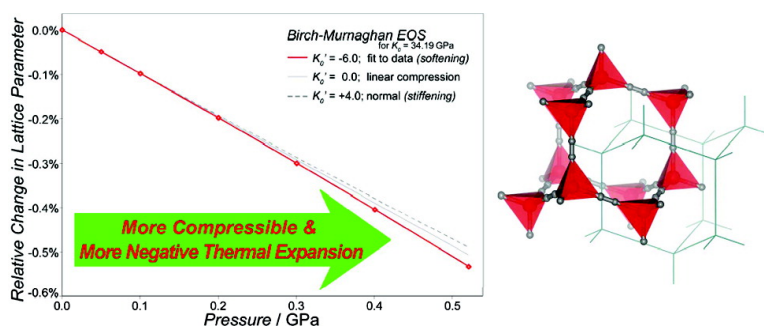


Pressure Enhancement of Negative Thermal Expansion Behavior and Induced Framework Softening in Zinc Cyanide

Karena W. Chapman, and Peter J. Chupas

J. Am. Chem. Soc., 2007, 129 (33), 10090-10091 • DOI: 10.1021/ja073791e • Publication Date (Web): 26 July 2007

Downloaded from <http://pubs.acs.org> on February 15, 2009



More About This Article

Additional resources and features associated with this article are available within the HTML version:

- Supporting Information
- Links to the 5 articles that cite this article, as of the time of this article download
- Access to high resolution figures
- Links to articles and content related to this article
- Copyright permission to reproduce figures and/or text from this article

[View the Full Text HTML](#)



Pressure Enhancement of Negative Thermal Expansion Behavior and Induced Framework Softening in Zinc Cyanide

Karena W. Chapman* and Peter J. Chupas*

X-ray Science Division, Advanced Photon Source, Argonne National Laboratory, Argonne, Illinois 60439

Received May 25, 2007; E-mail: chapmank@aps.anl.gov; chupas@anl.gov

The flexibility of open framework network solids is associated with structural distortions in response to applied pressures. While such pressure-induced structural transitions are well understood for traditional oxide-based materials including dense mineral oxides and open framework zeolites,^{1,2} the pressure response of more extended coordination (or metal-organic) frameworks has yet to be explored.³ In such systems, the more open structure and complex connectivities are likely to enhance framework flexibility and yield more extreme and exotic pressure-dependent behavior. Moreover, novel pressure-induced behavior would be anticipated at more moderate pressures than for oxides: pressures such as are routinely encountered in practical applications. Consequently, understanding the impact pressure on the structure and functional properties of coordination framework systems is not only of fundamental interest but is relevant to their practical application. Here we explore pressure-dependent behavior of the zinc cyanide framework and uncover an unusual pressure-induced framework softening and enhancement of negative thermal expansion (NTE) behavior; phenomena linked to increased framework flexibility at high pressure.

Zinc cyanide, $\text{Zn}(\text{CN})_2$, is the classic coordination framework material used to originally outline the principles of rational design through self-assembly of molecular components: a concept now central to this field.⁴ The cubic ($Pn\bar{3}m$) structure is formed by $\text{Zn}(\text{C/N})_4$ tetrahedra linked linearly by cyanide bridges to form doubly interpenetrated diamond-type (or expanded α -cristobalite) networks (Figure 1). This framework is likely to be exceptionally "soft" and flexible owing to the existence of low-energy lattice vibrations^{5,6} involving transverse displacement of the cyanide bridge.⁷ Thermal population of these modes underlies the NTE effect (a contraction upon heating), which has recently been identified in this and other cyanide-based framework materials.⁶⁻⁸

Lattice distortions induced at low pressure are likely to be related to these low-energy lattice vibrations and, thus, have the potential to influence the thermal expansion behavior.^{9,10} For the widely studied NTE oxide $\alpha\text{-ZrW}_2\text{O}_8$,¹¹ which at ambient pressure exhibits the largest isotropic NTE effect in an oxide-based system ($\alpha = dT/dl = -9.1 \times 10^{-6} \text{ K}^{-1}$), an irreversible (at 298 K) structural transition upon compression to 0.2 GPa virtually eliminates the NTE effect ($\alpha = -1.0 \times 10^{-6} \text{ K}^{-1}$).⁹ Pressure-induced transitions of this type are clearly detrimental to applications of NTE materials, which most significantly include compensating for "normal" (positive) thermal expansion in other materials such as within composites.¹² Such applications subject the material to low-grade pressures (up to ~ 1 GPa), through materials processing and intrinsic to the composite microstructure (e.g., strain from disparate atom stacking at interfaces in lamellar composites; intergranular stress between particles in three-dimensional composites). The additional flexibility associated with a double (CN) rather than single atom (O) bridge, which enhances NTE in cyanide-based systems,⁷ may also produce more exotic behavior under pressure.

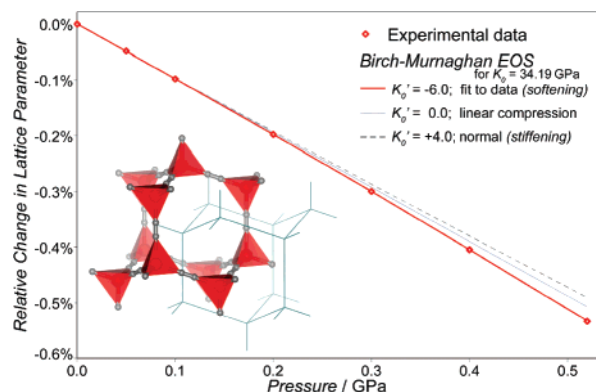


Figure 1. The behavior of $\text{Zn}(\text{CN})_2$ upon compression to 0.52 GPa. The equation of state (EOS) fit to the data and reference EOS are shown. The errors bars are within the data symbols. Inset: The $\text{Zn}(\text{CN})_2$ structure is shown, highlighting the Zn^{II} tetrahedra for one interpenetrated network.

Variable pressure and temperature time-of-flight neutron powder diffraction data for $\text{Zn}(\text{CN})_2$ were collected in a helium gas pressure apparatus¹³ within a dispex using the SEPD beamline at the Intense Pulsed Neutron Source, Argonne National Laboratory. The pressure apparatus applied precisely controlled, accurate, hydrostatic sample pressures upon compression to 0.52 GPa at ambient temperature and between 50 and 300 K under 0.2 and 0.4 GPa applied pressure. The cell geometry and collimation minimized contributions from the sample environment to the measured scattering to yield high-quality diffraction data.

Rietveld refinement¹⁴ of the diffraction data showed a continuous contraction of the cubic lattice parameter by $\sim 0.5\%$ between 0 and 0.52 GPa at constant temperature (Figure 1). This corresponds to the thermal contraction (i.e., NTE) evident over a 300 K range.⁷ The bulk modulus and its pressure dependence ($K_0 = 34.19(21)$ GPa, $K_0' = -6.0(7)$) at ambient temperature were determined by fitting a third-order Birch–Murnaghan (B–M) EOS¹⁵⁻¹⁷ to the pressure-induced changes in cell volume.

While conventional solids undergo pressure-induced stiffening, becoming less compressible at high pressure with a positive pressure dependence of the bulk modulus (typically $K_0' \sim 4$),¹⁸ distinctly different behavior is evident here. Indeed, $\text{Zn}(\text{CN})_2$ becomes progressively more compressible with increasing pressure over the range measured—a pressure-induced softening—with an anomalous (negative) value of K_0' . Although pressure-induced softening can be apparent near phase transitions, the fit here is consistent down to low pressure, and further compression to ~ 1.0 GPa did not reveal any phase transitions.

Variable temperature diffraction data collected at constant pressure show that the NTE behavior in $\text{Zn}(\text{CN})_2$ is not only retained in this pressure range but also increases with increasing pressure (Figure 2). The average coefficients of thermal expansion (α), obtained from least-square linear fits to the data, vary by ca. $-1 \times 10^{-6} \text{ K}^{-1}$ per 0.2 GPa from $-17.40(18) \times 10^{-6} \text{ K}^{-1}$ at ambient

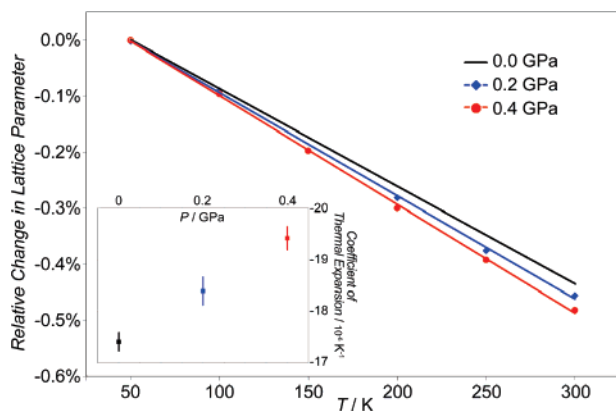


Figure 2. The thermal expansion behavior of $\text{Zn}(\text{CN})_2$ under pressure.

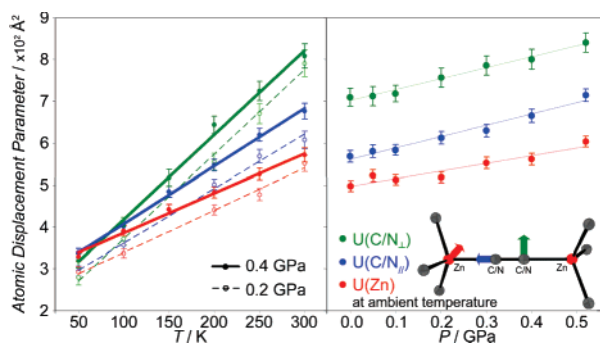


Figure 3. The temperature (right) and pressure (left) dependence of the atomic displacement parameters for $\text{Zn}(\text{CN})_2$.

pressure¹⁹ to $-18.39(27) \times 10^{-6}$ and $-19.42(23) \times 10^{-6} \text{ K}^{-1}$ at 0.2 and 0.4 GPa, respectively.

The refined structural models show that while the greatest increases in the atomic displacement parameters (ADPs) with heating occur for the C/N component perpendicular to the $\text{Zn} \cdots \text{Zn}'$ direction, as is consistent with the thermal population of transverse vibrational modes of the cyanide bridge,⁷ all ADPs increase approximately evenly upon compression (Figure 3). This suggests that additional lattice distortions are accessed at pressure: modes which are not significantly populated thermally.

In this low-pressure regime, compression is principally associated with increased bending distortion of the lattice from the perfect diamond topology with linear $\text{Zn}-\text{CN}-\text{Zn}'$ coordination, with only minor contribution from compression of the comparatively stiff, individual bonds. This may perturb the coordination bonding to enhance the bending flexibility of the $\text{Zn}-\text{CN}-\text{Zn}'$ units and, accordingly, the framework. Such softening of low-energy lattice vibrations under pressure has been documented in some oxide-based NTE materials.²⁰ Here, dynamic and static bending distortions of the $\text{Zn}-\text{CN}-\text{Zn}'$ moiety are involved in the thermal expansion and compression mechanisms, and hence, variations in flexibility of this unit have the potential to impact both properties. Enhanced flexibility (i.e., lower-energy vibrational modes) allows more rapid population of the lattice modes contributing to NTE, yielding the pressure enhancement of NTE behavior. At non-zero temperature, where modes associated with NTE are populated, the integrated effect of pressure-enhanced NTE would contribute to the measured volume contraction with pressure. Indeed, at lower temperatures, less pronounced framework softening may be evident. In addition, enhanced flexibility may facilitate further compression and also contribute to the observed pressure-induced framework softening.

The present investigation of $\text{Zn}(\text{CN})_2$ represents the first in situ structural study of a coordination framework material under pressures relevant to practical applications. Unlike the NTE oxide $\alpha\text{-ZrW}_2\text{O}_8$, no transformations detrimental to applications were evident for $\text{Zn}(\text{CN})_2$ in the low-pressure regime. Instead, novel compression behavior was observed with an anomalous pressure-induced framework softening and pressure enhancement of the NTE effect. We suspect that high-precision measurements may reveal similar effects in other NTE materials.²¹ Moreover, equally exotic high-pressure behavior is anticipated for other coordination frameworks, an expectation supported by the dramatic structural transitions that have been observed upon removal or exchange of guest species, which correlates to changes in internal pressure.²²

Acknowledgment. Work done at Argonne was supported by the U.S. DoE, Office of Science, Office of Basic Energy Sciences, under Contract No. DE-AC02-06CH11357. We thank J. A. Hriljac, J. B. Parise, and J. D. Jorgensen for useful discussions, and R. B. Von Dreele and J. Fieramosca for instrumental support.

Supporting Information Available: Details of neutron diffraction experiment, Rietveld refinements, and EOS fits. This material is available free of charge via the Internet at <http://pubs.acs.org>.

References

- (1) See, for example: (a) Hazen, R. M.; Prewitt, C. T. *Am. Mineral.* **1977**, *62*, 309–315. (b) Dove, M. T. *Am. Mineral.* **1997**, *82*, 213–244. (c) Richet, P.; Gillet, P. *Eur. J. Mineral.* **1997**, *9*, 907–933.
- (2) (a) Hazen, R. M. *Science* **1983**, *219*, 1065–1067. (b) Hriljac, J. A. *Crystallogr. Rev.* **2006**, *12*, 181–193.
- (3) Pressure-dependent magnetic properties have been explored for some systems; see, for example: (a) Garcia, Y.; van Koningsbruggen, P. J.; Lapouyade, R.; Fournes, L.; Rabardel, L.; Kahn, O.; Ksenofontov, V.; Levchenko, G.; Gutlich, P. *Chem. Mater.* **1998**, *10*, 2426–2433. (b) Moritomo, Y.; Hanawa, M.; Ohishi, Y.; Kato, K.; Takata, M.; Kuriki, A.; Nishibori, E.; Sakata, M.; Ohkoshi, S.; Tokoro, H.; Hashimoto, K. *Phys. Rev. B* **2003**, *68*, 144106.
- (4) Hoskins, B. F.; Robson, R. *J. Am. Chem. Soc.* **1990**, *112*, 1546–1554.
- (5) Chapman, K. W.; Hagen, M.; Kepert, C. J.; Manuel, P. *Physica B* **2006**, *385*, 60–62.
- (6) (a) Goodwin, A. L.; Kepert, C. J. *Phys. Rev. B* **2005**, *71*, 140301. (b) Goodwin, A. L. *Phys. Rev. B* **2006**, *74*, 134302.
- (7) Chapman, K. W.; Chupas, P. J.; Kepert, C. J. *J. Am. Chem. Soc.* **2005**, *127*, 15630–15636.
- (8) (a) Goodwin, A. L.; Chapman, K. W.; Kepert, C. J. *J. Am. Chem. Soc.* **2005**, *127*, 17980–17981. (b) Chapman, K. W.; Chupas, P. J.; Kepert, C. J. *J. Am. Chem. Soc.* **2006**, *128*, 7009–7014. (c) Pretsch, T.; Chapman, K. W.; Halder, G. J.; Kepert, C. J. *Chem. Commun.* **2006**, 1857–1859.
- (9) Evans, J. S. O.; Hu, Z.; Jorgensen, J. D.; Argyriou, D. N.; Short, S.; Sleight, A. W. *Science* **1997**, *275*, 61–65.
- (10) Lind, C.; VanDerveer, D. G.; Wilkinson, A. P.; Chen, J. H.; Vaughan, M. T.; Weidner, D. J. *Chem. Mater.* **2001**, *13*, 487–490.
- (11) Evans, J. S. O.; David, W. I. F.; Sleight, A. W., *Acta Crystallogr. Sect. B: Struct. Sci.* **1999**, *55*, 333–340.
- (12) Evans, J. S. O. *J. Chem. Soc., Dalton Trans.* **1999**, 3317–3326.
- (13) Jorgensen, J. D.; Pei, S.; Lightfoot, P.; Hinks, D. G.; Veal, B. W.; Dabrowski, B.; Paulikas, A. P.; Kleb, R.; Brown, I. D. *Physica C* **1990**, *171*, 93–102.
- (14) Larson, A. C.; Von Dreele, R. B., General Structure Analysis System (GSAS) 2000, Los Alamos National Laboratory Report, LAUR 86-748.
- (15) Angel, R. J. Equations of state. In *High-pressure and high-temperature crystal chemistry: Reviews in Mineralogy and Geochemistry*, Hazen, R. M., Downs, R.T., Eds.; 2000, *41*, 35–60.
- (16) Birch, F. *Phys. Rev.* **1947**, *71*, 809.
- (17) A high-quality EOS fit to relatively few data was enabled by the precise, accurate, hydrostatic pressures only possible with the gas pressure cell. EOS fit to subsets of this data and to a separate larger P–V data set, collected at finer pressure intervals with reduced signal-to-noise ratio, agreed within the precision of the fits (see Supporting Information).
- (18) Indeed, truncation of the B–M EOS to the second-order implies $K_0' = 4$.
- (19) From least-squares linear fit to data in ref 6 over 100–300 K.
- (20) (a) Ravindran, T. R.; Arora, A. K.; Mary, T. A. *Phys. Rev. Lett.* **2000**, *85*, 225–225. (b) Ravindran, T. R.; Arora, A. K.; Mary, T. A. *Phys. Rev. B* **2003**, *67*, 064301.
- (21) Pantea, C.; Migliori, A.; Littlewood, P. B.; Zhao, Y.; Ledbetter, H.; Lashley, J. C.; Kimura, T.; Duijn, J. V.; Kowach, G. R. *Phys. Rev. B* **2006**, *73*, 214118.
- (22) Halder, G. J.; Kepert, C. J. *Aust. J. Chem.* **2006**, *59*, 597–604.

JA073791E